Rapid and profound rewiring of brain lipid signaling networks by acute diacylglycerol lipase inhibition

Daisuke Ogasawara[a,1], Hui Deng[b,1], Andreu Viader[a], Marc P. Baggelaar[b], Arjen Breman[b], Hans den Dulk[b], Adriann M. C. H. van den Nieuwendijk[c], Marjolein Soethoudt[b], Tom van der Wel[b], Juan Zhou[b], Herman S. Overkleeft[c], Manuel Sanchez-Alavez[a], Simone Mo[a], William Nguyen[a], Bruno Conti[a], Xiaojie Liu[d], Yao Chen[d], Qing-song Liu[d], Benjamin F. Cravatt[a,2], and Mario van der Stelt[b,2]

[a]Department of Chemical Physiology, The Scripps Research Institute, La Jolla, CA 92037; [b]Department of Molecular Physiology, Leiden Institute of Chemistry, Leiden University, 2333 CC Leiden, The Netherlands; [c]Department of Bio-organic Synthesis, Leiden Institute of Chemistry, Leiden University, 2333 CC Leiden, The Netherlands; and [d]Department of Pharmacology and Toxicology, Medical College of Wisconsin, Milwaukee, WI 53226

This contribution is part of the special series of Inaugural Articles by members of the National Academy of Sciences elected in 2014.

Contributed by Benjamin F. Cravatt, November 13, 2015 (sent for review October 23, 2015; reviewed by Christopher Fowler and Stephan Sieber)

Diacylglycerol lipases (DAGLα and DAGLβ) convert diacylglycerol to the endocannabinoid 2-arachidonoylglycerol. Our understanding of DAGL function has been hindered by a lack of chemical probes that can perturb these enzymes in vivo. Here, we report a set of centrally active DAGL inhibitors and a structurally related control probe and their use, in combination with chemical proteomics and lipidomics, to determine the impact of acute DAGL blockade on brain lipid networks in mice. Within 2 h, DAGL inhibition produced a striking reorganization of bioactive lipids, including elevations in DAGs and reductions in endocannabinoids and eicosanoids. We also found that DAGLα is a short half-life protein, and the inactivation of DAGLs disrupts cannabinoid receptor-dependent synaptic plasticity and impairs neuroinflammatory responses, including lipopolysaccharide-induced anapyrexia. These findings illuminate the highly interconnected and dynamic nature of lipid signaling pathways in the brain and the central role that DAGL enzymes play in regulating this network.

endocannabinoid | lipase | inhibitor | nervous system

Classically understood forms of neurotransmission involve polar small molecules that are stored in synaptic vesicles and released in response to depolarizing signals that promote vesicle fusion with the presynaptic plasma membrane of neurons (1). More recently, lipids have become recognized as a distinct type of chemical messenger in the nervous system that appear to be generated at the time of their intended action rather than amassed in vesicles (2–5). This "on-demand" model for production implicates lipid biosynthetic enzymes as major regulators of chemical signaling in the central nervous system (CNS). In support of this premise, the enzymes that produce several classes of lipid transmitters, including lysophospholipids (6), eicosanoids (7), and endocannabinoids (8, 9), are highly expressed in the nervous system and play important roles in brain development, synaptic plasticity, and the modulation of complex behaviors. For example, the diacylglycerol (DAG) lipase enzymes DAGLα and DAGLβ (10) produce the endocannabinoid 2-arachidonoylglycerol (2-AG) (11, 12), and the constitutive genetic disruption of DAGLα lowers brain 2-AG and arachidonic acid (AA) content (13, 14), resulting in impaired synaptic plasticity (13, 14), hypophagia (15), enhanced anxiety and fear responses (16, 17), and propensity for spontaneous seizures (15).

Many bioactive lipids share structural features and can be, in principle, connected to one another through multistep metabolic routes (2, 18, 19), suggesting the potential for cross-talk among lipid signaling pathways in vivo. Such cross-talk could produce more sophisticated forms of integrated or counter-balanced signal transduction to affect complex physiological or disease processes in a dynamic manner. The extent to which individual enzymes within larger metabolic pathways exert control over a multitude of bioactive lipids, however, remains poorly understood. This question can be studied in genetically modified mice lacking specific lipid metabolic enzymes, but the long-term, constitutive inactivation of enzymes renders these models poorly suited for distinguishing rapid and dynamic processes from slower, adaptive changes that may occur in lipid pathways. Pharmacological approaches, on the other hand, provide a powerful means to assess the temporal consequences of acute enzyme blockade on the dynamic composition of lipid networks in the brain under both physiological and pathological conditions. Unfortunately, selective and in vivo active inhibitors are not yet available for many lipid biosynthetic enzymes. Known inhibitors for DAGLs, for example, have been used to study the function of 2-AG as a retrograde messenger in neuronal cell and brain slice preparations (20–25), but these inhibitors lack the selectivity (26), potency, and chemical properties (21) required for central activity in vivo.

Significance

Lipid transmitters, such as endocannabinoid and eicosanoids, play important roles in the nervous system and regulate behaviors that include pain, emotionality, and addiction. Chemical probes that perturb lipid transmitter biosynthesis are needed to understand the functions of these pathways in the nervous system. Here, we describe selective and in vivo active inhibitors of the diacylglycerol lipases DAGLα and DAGLβ, which biosynthesize the endocannabinoid 2-arachidonoylglycerol (2-AG). We show that these inhibitors produce rapid and dramatic changes in a brain lipid signaling network, comprising not only 2-AG, but also eicosanoids and diacylglycerols. These lipid changes are accompanied by impairments in synaptic plasticity and attenuation of neuroinflammatory responses in vivo, underscoring the broad role that DAGLs play in nervous system metabolism and function.

Author contributions: D.O., H.D., A.V., H.S.O., B.C., Q.-s.L., and M.v.d.S. designed research; D.O., H.D., A.V., M.P.B., A.B., H.d.D., A.M.C.H.v.d.N., M.S., T.v.d.W., J.Z., M.S.-A., S.M., W.N., X.L., and Y.C. performed research; D.O., H.D., M.P.B., A.B., H.d.D., A.M.C.H.v.d.N., M.S., T.v.d.W., J.Z., M.S.-A., S.M., W.N., X.L., and Y.C. contributed new reagents/analytic tools; D.O., H.D., A.V., M.P.B., A.B., H.d.D., A.M.C.H.v.d.N., M.S., T.v.d.W., J.Z., H.S.O., M.S.-A., S.M., W.N., B.C., X.L., Y.C., Q.-s.L., B.F.C., and M.v.d.S. analyzed data; and D.O., H.D., A.V., H.d.D., H.S.O., B.C., Q.-s.L., B.F.C., and M.v.d.S. wrote the paper.

Reviewers: C.F., Umea University; and S.S., Technical University of Munich.

Conflict of interest statement: B.F.C. is a founder and advisor to Abide Therapeutics, a biotechnology company interested in developing serine hydrolase inhibitors as therapeutics.

[1]D.O. and H.D. contributed equally to this work.

[2]To whom correspondence may be addressed. Email: cravatt@scripps.edu or m.van.der.stelt@chem.leidenuniv.nl.

This article contains supporting information online at www.pnas.org/lookup/suppl/doi:10.1073/pnas.1522364112/-/DCSupplemental.

Here, we describe the synthesis and characterization of CNS-active, covalent 1,2,3-triazole urea inhibitors of DAGLα and -β that, when paired with a structurally related control compound and tailored activity-based probes, provide a suite of chemical tools for investigating DAGL function in vivo. We show that acute pharmacological blockade of DAGL leads to a rapid and dramatic reorganization of lipid signaling pathways in the brain that includes elevations in bioactive DAGs and reductions in the two major endocannabinoids [2-AG and *N*-arachidonoylethanolamine (anandamide or AEA)], arachidonic acid, and the prostaglandins PGD_2 and PGE_2. DAGL inhibitors also impair endocannabinoid-dependent forms of synaptic plasticity and attenuate lipopolysaccharide-induced neuroinflammatory responses, including reductions in core body temperature (anapyrexia). These findings highlight the special role that DAGL enzymes play as integrative nodes for coordinating cross-talk among several classes of lipid transmitters to modulate neuro(immuno)logical functions in the CNS.

Results

Potent and Selective 1,2,3-Triazole Urea Inhibitors of DAGLα. The development of DAGL inhibitors has been historically hindered by a dearth of assays for monitoring the activity of these enzymes in native biological systems. We have recently introduced tailored activity-based probes that enable the independent and concurrent monitoring of DAGLα and DAGLβ activities in the brain and other tissue/cell types (27, 28). Guided by competitive activity-based protein profiling (ABPP) methods (29), we converted one of these tailored probes into a series of potent 1,2,3-triazole urea (1,2,3-TU) inhibitors of DAGLβ that displayed peripheral, but not central activity in vivo (27) [e.g., KT172 (**1**)] (Fig. 1*A*). Here, we set out to further modify and optimize the 1,2,3-TU scaffold to generate selective and CNS-active inhibitors of DAGLα and -β. We discovered, in brief, that modifications to the distal phenyl ring appended to the triazole leaving group of KT172 yielded inhibitors (e.g., DO6, DO13) with good potency for DAGLα and moderate inhibition of DAGLβ (*SI Appendix*, Fig. S1), but the resulting compounds showed little or no CNS activity in vivo. We therefore turned our attention to modifying the staying group of the 1,2,3-TU scaffold (Fig. 1*A*, blue), which, in combination with truncated extensions of the triazole leaving group (Fig. 1*A*, black), furnished two structurally distinct compounds—DH376 (**4**) and DO34 (**5**)—as highly potent DAGL inhibitors (Fig. 1*A*). DH376 and DO34 blocked the DAGLα conversion of 1-stearoyl-2-arachidonoyl-*sn*-glycerol (SAG) to 2-AG with IC_{50} values of 6 nM [5–9 nM; 95% confidence interval (CI), $n = 4$] and 6 nM (3–11 nM 95% CI, $n = 4$), respectively (Fig. 1*B* and *SI Appendix*, Table S1), as determined using a real-time, fluorescence-based natural substrate assay with membrane lysates from HEK293T cells expressing recombinant human DAGLα (30). Using this substrate assay, we also confirmed that DH376 and DO34 were potent inhibitors of DAGLβ with IC_{50} values of 3–8 nM (Fig. 1*B* and *SI Appendix*, Table S1).

DH376 possesses a chiral propargyl ether at the C4 position of the staying group, which we surmised could serve as a handle to introduce reporter groups by copper-catalyzed azide-alkyne cycloaddition (CuAAC or "click") chemistry (31) to generate an additional class of DAGL-tailored activity-based probes for target engagement studies. With this goal in mind we synthesized a BODIPY-derivatized analog of DH376 termed DH379 (**6**) and confirmed that this probe labeled recombinant DAGLα and DAGLβ and detected these enzymes in the mouse brain membrane proteome (*SI Appendix*, Fig. S2).

We next used competitive ABPP assays to evaluate the activity and selectivity of DH376 and DO34 against endogenous DAGLs and other serine hydrolases in the mouse brain membrane proteome. We performed these studies with three different activity-based probes: two DAGL-tailored activity-based probes—DH379 (*SI Appendix*, Fig. S2) and HT-01 (27)—and a broad-spectrum serine hydrolase-directed probe fluorophosphonate-rhodamine (FP-Rh) (32). HT-01 and DH379 provided target engagement assays for DAGLs, and FP-Rh assessed cross-reactivity across a broad array of brain serine hydrolases. DH376 and DO34 inhibited DAGLα and -β labeling by DH379 (*SI Appendix*, Fig. S3 *A* and *B* and Table S1) and HT-01 (*SI Appendix*, Fig. S3 *C* and *D* and Table S1) with IC_{50} values in the range of 0.5–1.2 (DAGLα) and 2.3–4.8 (DAGLβ) nM, respectively. The IC_{50} values measured for DAGLα by competitive ABPP were ∼10-fold lower than those measured with the SAG substrate assay, which could reflect differences in the endogenous versus recombinant forms of this enzyme. DO34 and DH376 showed excellent selectivity for DAGLs, with the only detectable serine hydrolase off-targets being ABHD6 and PLA2G7 (*SI Appendix*, Fig. S3). Finally, DH376 and DO34 showed

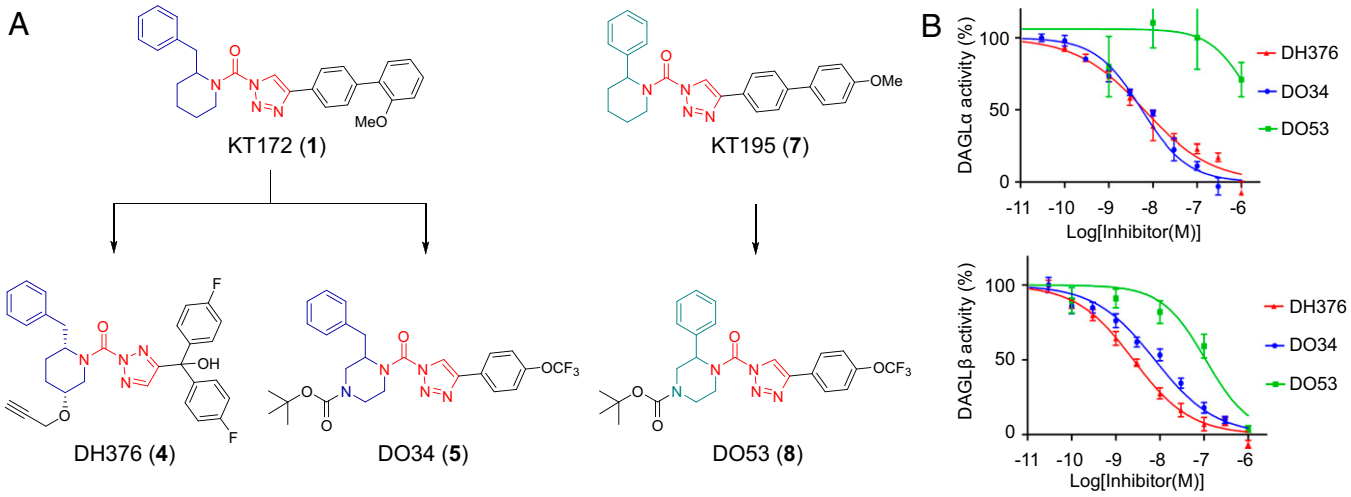

Fig. 1. Discovery of 1,2,3-TU inhibitors (DH376, DO34) and a control probe (DO53) for DAGLs. (*A*) Chemical structures of original DAGL inhibitor KT172 and structurally related control probe KT195 highlighting conserved features [blue (staying groups, KT172, DH376, DO34), red (triazole urea reactive groups), green (staying groups, KT195 and DO53)] and modifications (black) that furnished potent DAGL inhibitors DH376 and DO34 and the control probe DO53. (*B*) Concentration-dependent inhibition of recombinant human DAGLα and mouse DAGLβ activity by DH376, DO34, and DO53 as measured with a SAG substrate assay in DAGL-transfected HEK293T cells (30). Data represent average values ± SD; $n = 4$ per group.

minimal and negligible binding, respectively, to cannabinoid CB_1 (CB_1R) and CB_2 (CB_2R) receptors as measured with radioligand binding assays (IC_{50} values > 1 μM) (*SI Appendix*, Fig. S4).

We have previously shown that 2-phenyl piperidine analogs, such as KT195 (**7**) (Fig. 1*A*), serve as useful inactive control probes that display greatly attenuated inhibition of DAGLs, while maintaining activity against common off-targets like ABHD6 (27). Based on this precedent, we synthesized DO53 (**8**), a 2-phenyl piperazine analog of DO34, and found that this agent exhibited ∼100-fold lower activity against DAGLα compared with DO34 or DH376 as measured by DAG substrate hydrolysis (Fig. 1*B* and *SI Appendix*, Table S1) or competitive ABPP assays in mouse brain (*SI Appendix*, Fig. S3 and Table S1). On the other hand, DO53 cross-reacted with the shared off-targets of DO34 and DH376 (*SI Appendix*, Fig. S3), designating DO53 as a potentially suitable control compound for biological studies of DAGL enzymes.

DAGLα Inhibitors Are Centrally Active in Vivo. We administered DH376, DO34, DO53, or vehicle intraperitoneally to male C57BL/6 mice across a dose range of 3–50 mg/kg. After 4 h, the animals were sacrificed and brain tissue analyzed by competitive ABPP with DH379, HT-01, and FP-Rh, which revealed clear dose-dependent blockade of DAGLα activity for both DH376 and DO34 with ED_{50} values of 5–10 mg/kg (Fig. 2 *A* and *B* and *SI Appendix*, Fig. S5), and full inhibition of the enzyme being observed at 30–50 mg/kg of inhibitor. DAGLβ (and ABHD6) were also inhibited by DH376, and to a lesser extent by DO34, which instead exhibited cross-reactivity with PLA2G7 (Fig. 2 *A* and *B* and *SI Appendix*, Fig. S5). DO53, on the other hand, did not substantially inhibit DAGLα or -β at any dose tested (Fig. 2*C* and *SI Appendix*, Fig. S5), but inhibited both ABHD6 and PLA2G7 (Fig. 2*C* and *SI Appendix*, Fig. S5). We conjugated brain proteomes from DH376-treated mice to a Cy5 fluorophore by CuAAC, which confirmed direct, dose-dependent labeling of DAGL enzymes (*SI Appendix*, Fig. S5 *E–G*).

We confirmed and extended these target engagement profiles by performing ABPP coupled to high-resolution, quantitative mass spectrometry (MS). In brief, brain proteomes from inhibitor- and vehicle-treated mice were incubated with the serine hydrolase-directed activity-based probe FP-biotin (33), and probe-labeled enzymes were enriched by streptavidin chromatography, digested on bead with trypsin, and the resulting tryptic peptides modified by reductive dimethylation (ReDiMe) of lysine residues using isotopically heavy and light formaldehyde, respectively (34). In these experiments, inhibited serine hydrolases are identified as enzymes showing low heavy/light ReDiMe ratios. Quantitative MS confirmed complete inhibition of DAGLα by DH376 and DO34, with DAGLβ also being strongly and partially inhibited by these compounds, respectively, and revealed the following off-targets (defined as serine hydrolases with heavy/light ratios < 0.5): ABHD6

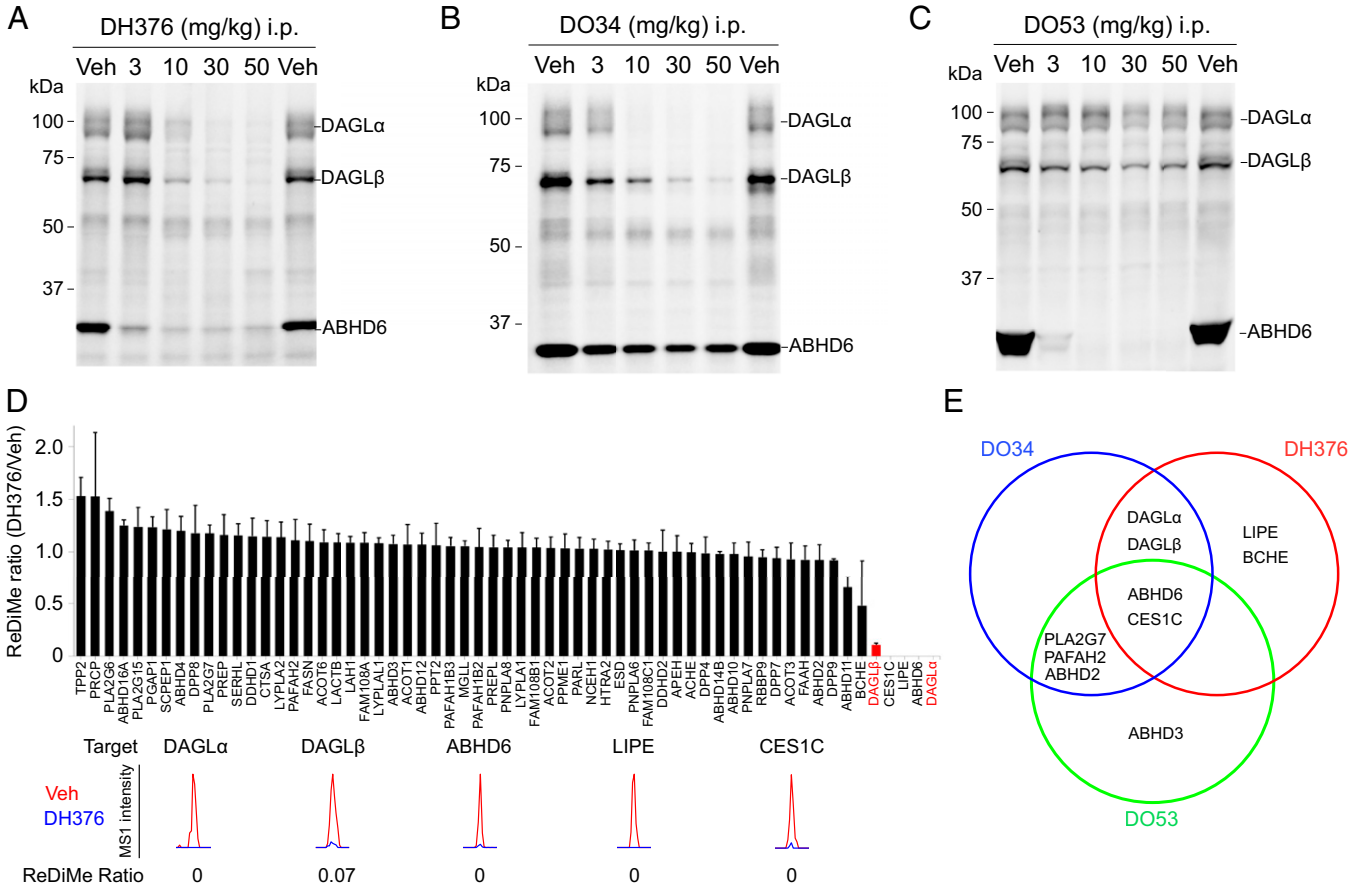

Fig. 2. In vivo activity and selectivity of DH376, DO34, and DO53 in mice. (*A–C*) Dose-dependent inhibition of DAGLα and DAGLβ in brain tissue from mice treated with DH376 (*A*), DO34 (*B*), and DO53 (*C*) (indicated doses, intraperitoneal, 4-h treatment) as determined by competitive ABPP using the DH379 probe (1 μM, 30 min). (*D*) ABPP-ReDiMe analysis of brain serine hydrolase activities from mice treated with DH376 (50 mg/kg, i.p., 4-h treatment), where serine hydrolases were labeled and enriched using an FP-biotin probe (33). Representative MS1 chromatograms for DAGLα and DAGLβ, as well as additional serine hydrolase targets are shown. Data represent average values ± SEM; $n = 4$ mice per group. (*E*) Summary of the serine hydrolase targets of DH376, DO34, and DO53 in mouse brain. Serine hydrolases with ReDiMe ratio values < 0.5 were defined as targets for each inhibitor. Note that the DAGLα and DAGLβ are the only two serine hydrolases found to be inhibited by both DH376 and DO34, but not DO53, in mouse brain.

(DH376, DO34), CES1C (DH376, DO34), ABHD2 (DO34), BCHE (DH376), LIPE (DH376), PAFAH2 (DO34), and PLA2G7 (DO34) (Fig. 2*D*, *SI Appendix*, Fig. S6*A*, and Dataset S1). DO53 showed negligible activity against DAGLα or β (heavy/light ratios of ∼0.8), but cross-reacted with many of the off-targets of DH376 and DO34 (ABHD2, ABHD6, CES1C, PLA2G7, PAFAH2) (*SI Appendix*, Fig. S6*B* and Dataset S1). Taken together (Fig. 2*E*), these competitive ABPP studies designated DH376 and DO34 as in vivo-active inhibitors with complementary selectivity profiles that, when used in combination with the control probe DO53, can report on the function of DAGLs in the CNS.

We next investigated the time course of DAGL inhibition in mice. At a high dose (50 mg/kg), DH376 and DO34, but not DO53, demonstrated sustained inhibition of DAGLs for up to 8 h, with partial recovery at 24-h postdosing (Fig. 3*A* and *SI Appendix*, Fig. S5*C*). Interestingly, a lower dose of DH376 (3 mg/kg) produced substantial inhibition of DAGLα within 30 min after administration, but enzyme activity quickly recovered by 4 h (Fig. 3 *B* and *C*). In contrast, DAGLβ was only partly inhibited at 3 mg/kg (Fig. 3*B*), whereas the off-target ABHD6 remained inhibited up to 8 h (Fig. 3 *B* and *C*). We confirmed these differences in the duration of target engagement by ex vivo CuAAC-mediated conjugation of a Cy5-azide tag to brain proteomes of DH376-treated mice, which showed strong, but transient DH376 labeling of DAGLα and sustained reactivity with ABHD6 (Fig. 3 *D* and *E*). The recovery of DAGLα activity in this time-course study at low drug dose could indicate that DAGLα is a short half-life protein that is rapidly degraded and replaced by newly synthesized enzyme or that the DH376–DAGLα interaction is reversible. Arguing against the latter hypothesis, however, we found that the inhibition and direct labeling of DAGLα by DH376 were maintained after size-exclusion chromatography, which contrasted with the substantial rescue of DAGLα activity observed in this experiment with the reversible inhibitor LEI105 (25) (*SI Appendix*, Fig. S7). DH376, but not LEI105, also showed a time-dependent increase in potency against DAGLα and, following preincubation, was not outcompeted by excess substrate (*SI Appendix*, Fig. S7), additional hallmarks of an irreversible mechanism of action. Our results thus support that DAGLα is a short half-life protein in the CNS and further demonstrate that sustained inhibition of DAGLα for many hours can be achieved at higher doses of DH376 and DO34 (50 mg/kg), where presumably sufficient drug remains in the CNS to block newly synthesized DAGLα protein.

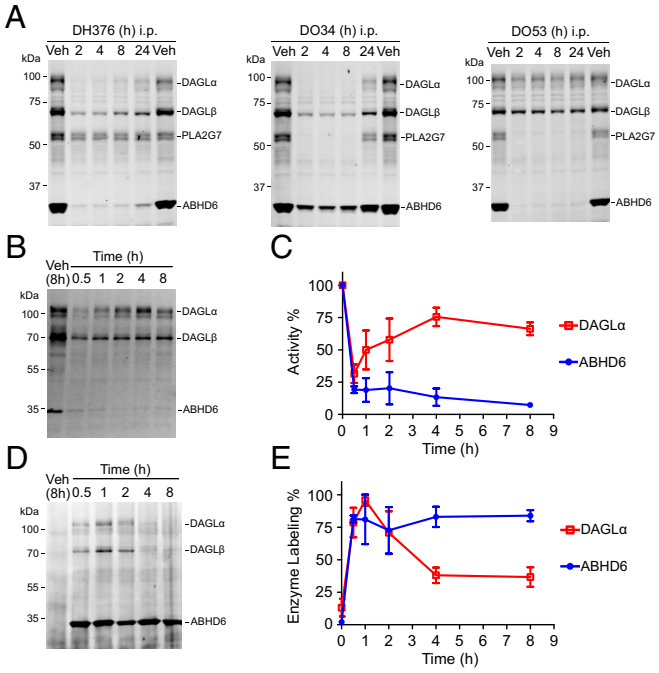

Fig. 3. Time-course analysis of DAGLα inhibition and recovery. (*A*) Time course of inhibition of DAGLα in brain tissue from mice treated with vehicle (Veh) or DH376, DO34, and DO53 (50 mg/kg, i.p.) as determined by competitive ABPP using the DH379 probe (1 μM, 30 min). (*B* and *C*) Time course of inhibition of DAGLα in brain tissue from mice treated with a low dose of DH376 (3 mg/kg, i.p.) as determined by competitive ABPP using the DH379 probe (1 μM, 30 min). Gel data (*B*) and quantification of these data (*C*) relative to a vehicle-treated control group are shown for both DAGLα and ABHD6, an off-target of DH376. Data represent average values ± SEM; $n = 3$ mice per group. (*D* and *E*) Time course of direct labeling of DAGLα in brain tissue from mice treated with DH376 (3 mg/kg, i.p.) visualized by CuAAC to a Cy5 reporter group. Gel data (*D*) and quantification of these data (*E*) relative to a vehicle-treated control group are shown for both DAGLα and ABHD6. Data represent average values ± SEM; $n = 3$ mice per group.

DAGL Inhibitors Rapidly and Radically Alter Brain Lipid Profiles in Mice. Three independently generated lines of DAGLα$^{-/-}$ mice have shown that genetic disruption of this enzyme substantially reduces brain 2-AG (∼80–90%) (13, 14, 17). These brain 2-AG changes are accompanied by concomitant accumulation of the main 2-AG lipid precursor and protein kinase C (PKC) agonist (35) SAG (17) and depletion of the principal 2-AG hydrolytic metabolite and eicosanoid precursor AA (13, 14, 17), as well as of the second major endocannabinoid anandamide (AEA) (13, 14). It remains unclear, however, what portion of these widespread alterations reflects the active and dynamic regulation of brain lipid signaling networks by DAGLα versus adaptive changes caused by the constitutive, long-term ablation of this enzyme. We set out to address this important question by examining the brain lipid profiles of mice treated with the DAGL inhibitors DH376 and DO34 and the control probe DO53.

We first analyzed the brain lipid profiles of mice by LC-MS at a single 4-h time point postdosing with inhibitors (50 mg/kg, i.p.), which revealed dramatic reductions in 2-AG in DH376- and DO34- but not DO53-treated mice (Fig. 4*A* and Dataset S2). This reduction in 2-AG was comparable in magnitude to that observed in DAGLα$^{-/-}$ mice (Fig. 4*A* and Dataset S2), demonstrating the rapid flux of DAGL-mediated 2-AG production in vivo. The robust depletion of brain 2-AG in DH376- and DO34-treated mice was dose-dependent (*SI Appendix*, Fig. S8*A* and Dataset S2) and was observed within 2 h after injection (Fig. 4*B*, *SI Appendix*, Fig. S8*B*, and Dataset S2). The time-dependent changes in 2-AG caused by DH376 appeared to be shorter-lived than those of DO34 (Fig. 4*B*, *SI Appendix*, Fig. S8*B*, and Dataset S2). Notably, DH376 and DO34 also caused rapid, dose-dependent changes in other DAGL-regulated lipids, including reductions in AEA (Fig. 4 *C* and *D*, *SI Appendix*, Fig. S8, and Dataset S2), AA (Fig. 4 *E* and *F*, *SI Appendix*, Fig. S8, and Dataset S2), and the prostaglandins PGD_2 and PGE_2 (Fig. 4 *G*–*J*, *SI Appendix*, Fig. S8, and Dataset S2), as well as elevations in SAG (Fig. 4 *K* and *L*, *SI Appendix*, Fig. S8, and Dataset S2) and C18:1/C20:4 DAG (Dataset S2). The changes in each lipid species were again similar in magnitude to those observed in DAGLα$^{-/-}$ mice (Fig. 4 *C*, *E*, *G*, *I*, and *K*), were dose-dependent (*SI Appendix*, Fig. S8*A*), displayed similar time courses to alterations observed in 2-AG in DH376- and DO34-treated mice (Fig. 4 *D*, *F*, *H*, *J*, and *L*, and *SI Appendix*, Fig. S8*B*), and were absent in DO53-treated mice (Fig. 4 *C*, *E*, *G*, *I*, and *K*). Although most lipid changes were consistent between DAGL inhibitor-treated and DAGLα$^{-/-}$ mice, we did find that DAGLα$^{-/-}$ mice showed reductions in triglycerides, that were not observed in animals treated with DAGL inhibitors (Dataset S2). These alterations in triglycerides may thus require chronic, long-term inactivation of DAGLα, which is also known to cause significant reductions in total body weight and fat (15).

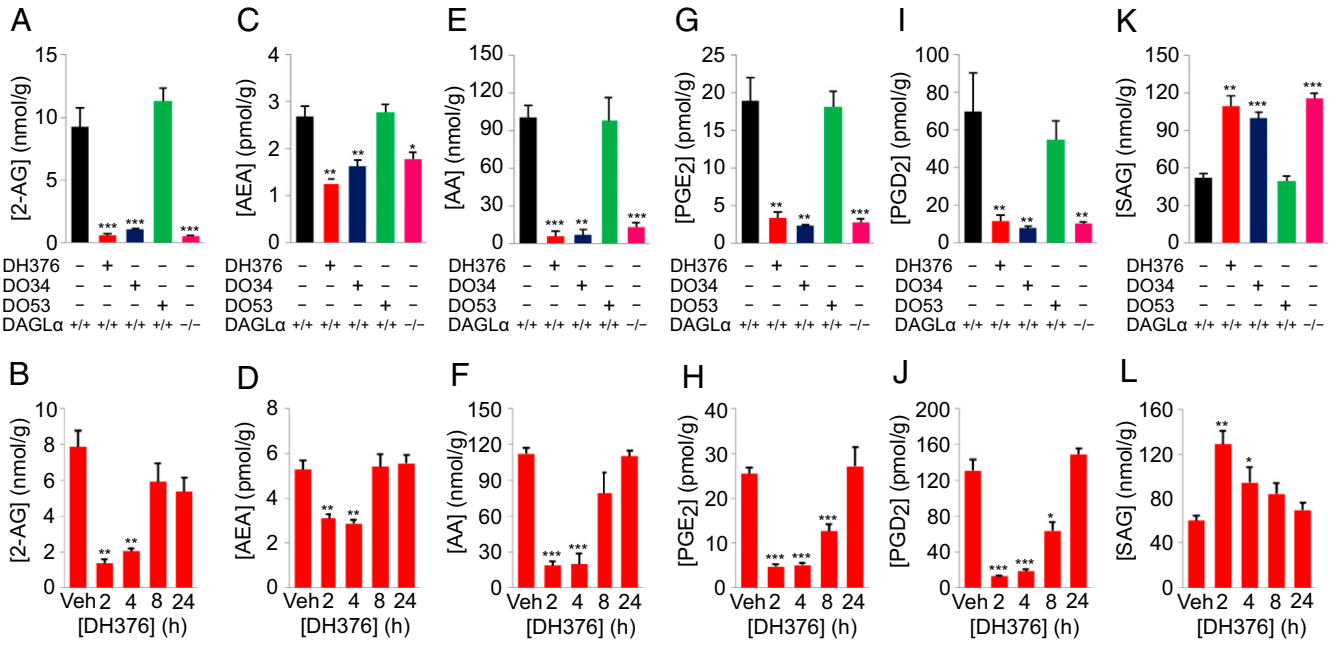

Fig. 4. Acute inhibition of DAGLs causes rapid and profound remodeling of bioactive lipid pathways in the brain. (*A*, *C*, *E*, *G*, *I*, *K*) Quantification of 2-AG (*A*) and related bioactive lipids (*C*, *E*, *G*, *I*, *K*) in brain tissue from mice treated with vehicle or DH376, DO34, and DO53 (50 mg/kg, i.p., 4 h). Lipid profiles from DAGLα$^{-/-}$ mice are shown for comparison. Data represent average values ± SEM; n = 5–6 mice per group. *P < 0.05; **P < 0.01; ***P < 0.001 for inhibitor-treated DAGLα$^{+/+}$ mice or DAGLα$^{-/-}$ mice vs. vehicle-treated DAGLα$^{+/+}$ mice. (*B*, *D*, *F*, *H*, *J*, *L*) Time-dependent changes in 2-AG (*B*) and bioactive lipids (*D*, *F*, *H*, *J*, *L*) in brain tissue from mice treated with DH376 (50 mg/kg, i.p.). Data represent average values ± SEM; n = 4–5 mice per group. *P < 0.05; **P < 0.01; ***P < 0.001 for inhibitor-treated vs. vehicle-treated mice.

These studies, taken together, demonstrate that acute pharmacological blockade of DAGLs produces a rapid and dramatic reorganization of lipid signaling networks in the mammalian brain that largely mirrors the myriad lipid changes observed in the brains of DAGLα$^{-/-}$ mice. Accordingly, we next asked whether DH376 and DO34 would affect physiological processes that involve one or more components of the DAGL-regulated lipid signaling network.

DAGL Inhibitors Block Endocannabinoid-Dependent Synaptic Plasticity. 2-AG functions as a major retrograde messenger at synapses throughout the brain that acts on presynaptically localized CB_1Rs to suppress neurotransmitter release (20). Various forms of synaptic plasticity are regulated by 2-AG signaling, including depolarization-induced suppression of excitation (DSE) and inhibition (DSI) (20), both of which are abolished in DAGLα$^{-/-}$ mice (13, 14). Interestingly, however, conflicting findings have emerged about whether the retrograde signaling 2-AG is biosynthesized by DAGLα on-demand or, alternatively, presynthesized and stored within neurons before stimulus-induced release (21–23, 25). As noted by others (21), these differences may reflect the poor physicochemical properties of the DAGL inhibitors used in past studies, as the high lipophilicity of these molecules could limit their penetration into brain tissue preparations used to measure DSI and DSE, resulting in incomplete inhibition of DAGLs. We therefore tested the effects of DH376, DO34, and DO53 in models of endocannabinoid-dependent synaptic plasticity.

We first examined DSE at parallel fiber (PF) to Purkinje cell (PC) synapses in acute cerebellar slices. A brief depolarization of PCs induced robust transient DSE at PF-PC synapses in vehicle-treated cerebellar slices (*SI Appendix*, Fig. S9*A*). Bath application of DH376 (1–10 μM) or DO34 (0.1–1 μM) to cerebellar slices 30 min before starting electrophysiological recordings blocked DSE in a concentration-dependent manner with a half-maximal inhibition of 1.1 μM and 0.18 μM, respectively (*SI Appendix*, Fig. S9 *A* and *B*). The control probe DO53 did not alter cerebellar DSE (10 μM) (*SI Appendix*, Fig. S9 *A* and *B*). We then evaluated DSI at CA1 pyramidal neuron synapses in hippocampal slices. DSI was induced in vehicle-treated hippocampal slices by applying a brief depolarization while evoking inhibitory postsynaptic currents through stimulation of synaptic inhibitory inputs (*SI Appendix*, Fig. S9*C*). Bath application of DH376 (10 μM) and DO34 (1 μM), but not DO53 (10 μM), for 30 min before starting electrophysiological recordings fully blocked hippocampal DSI (*SI Appendix*, Fig. S9 *C* and *D*).

These results support a model where the 2-AG that regulates both DSE and DSI forms of synaptic plasticity in the brain is produced on-demand by DAGLα.

DAGL Inhibitors Attenuate Neuroinflammatory Responses in Vivo. Monoacylglycerol lipase (MAGL or MGLL)-mediated hydrolysis of 2-AG provides a major source of AA substrate for prostaglandin synthesis in the nervous system under basal and neuroinflammatory states (36–39). Having discovered that acute, pharmacological inhibition of DAGLs coordinately lowers 2-AG and prostaglandin content of the brain (Fig. 4), we next asked whether blocking these enzymes affects neuroinflammatory processes regulated by these bioactive lipids. High-dose lipopolysaccharide (LPS) treatment induces brain prostaglandin and cytokine production (36, 39) and leads to profound anapyrexia in rodents (40, 41), an effect that is thought to be mediated, at least in part, by centrally produced prostaglandins and endocannabinoids (40). MAGL blockade has been shown to suppress LPS-induced prostaglandin and cytokine production in the CNS (36, 39), but also exacerbates the anapyrexia observed in this paradigm through a CB_1R-dependent mechanism (41). Building on these observations, we examined the effects of pharmacological and genetic inactivation of DAGL activity on neuroinflammatory responses induced by LPS.

Mice were treated with DH376, DO34, DO53 (50 mg/kg, i.p) or vehicle (60–90 min), followed by LPS (20 mg/kg, i.p., 6 h) or vehicle, and then sacrificed and their brain lipid and cytokine profiles analyzed. As expected, DH376- and DO34-treated mice, as well as DAGLα$^{-/-}$ mice but not DO53-treated mice, exhibited

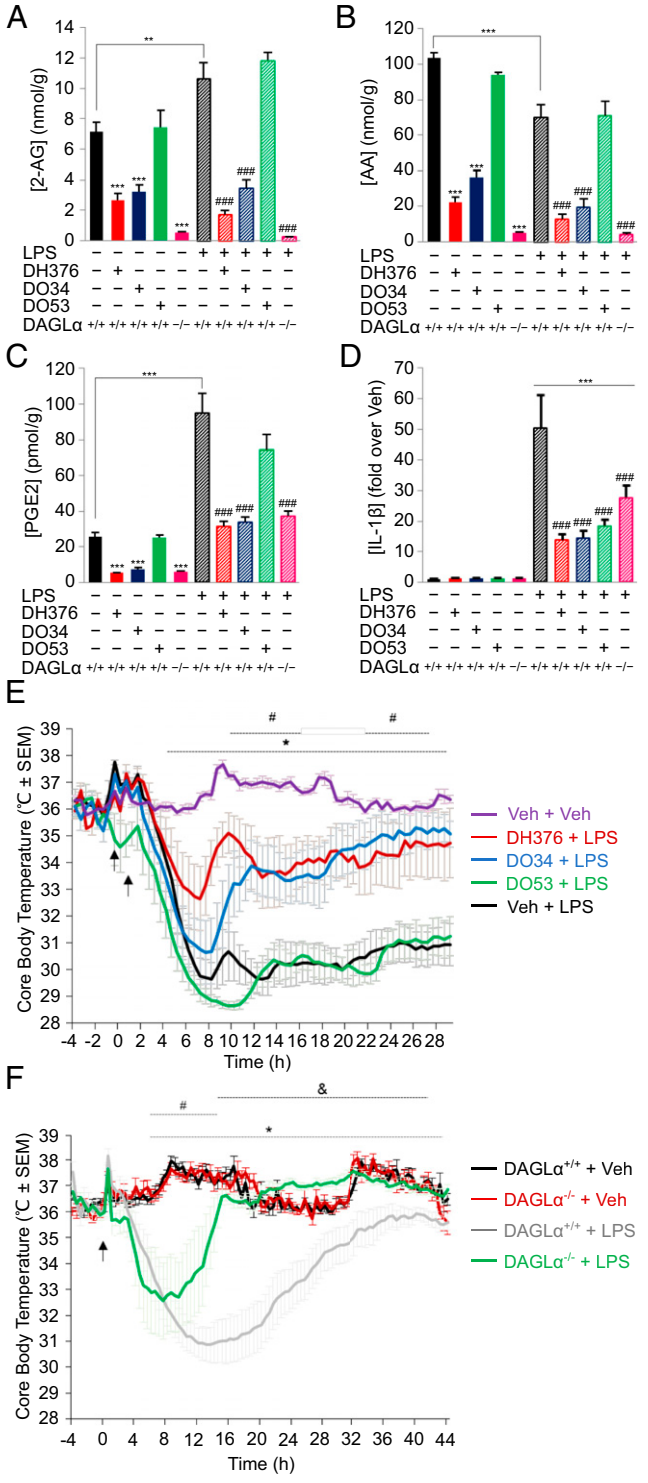

Fig. 5. Acute inhibition of DAGLs suppresses LPS-induced neuroinflammatory responses in mouse brain. (*A*–*C*) Quantification of 2-AG and related bioactive lipids in brain tissue from vehicle- or DH376-, DO34-, and DO53-treated (50 mg/kg, i.p., 1–1.5 h) or DAGLα$^{-/-}$ mice with or without subsequent treatment with LPS (20 mg/kg, i.p., 6 h). (*D*) Quantification of the IL-1β cytokine from DH376-, DO34-, and DO53-treated (50 mg/kg, i.p., 1–1.5 h) or DAGLα$^{-/-}$ mice with or without subsequent treatment with LPS (20 mg/kg, i.p., 6 h). Additional cytokine measurements are provided in *SI Appendix*, Fig. S10. For *A*–*D*, Data represent average values ± SEM; n = 5–8 mice per group. $^{**}P < 0.01$; $^{***}P < 0.001$ for all groups vs. vehicle-treated DAGLα$^{+/+}$ mice and $^{\#\#\#}P < 0.001$ for all groups compared with LPS-treated DAGLα$^{+/+}$ mice. (*E* and *F*) Time course of body temperature changes for mice pretreated with vehicle or DH376, DO34, and DO53 (*E*) or for DAGLα$^{+/+}$ and DAGLα$^{-/-}$ mice (*F*) following LPS treatment (10 mg/kg, i.p.). Data represent average values ± SEM; n = 5–6. For *E*, $^{*}P < 0.05$ Veh + Veh vs. Veh + LPS group; $^{\#}P < 0.05$ for DH376 + LPS and DO34 + LPS vs. Veh + LPS group. For *F*, $^{*}P < 0.05$ for DAGLα$^{+/+}$ + Veh vs. DAGLα$^{+/+}$ + LPS groups; $^{\#}P < 0.05$ for DAGLα$^{-/-}$ + Veh vs. DAGLα$^{-/-}$ + LPS groups; $^{\&}P < 0.05$ for DAGLα$^{-/-}$ + LPS vs. DAGLα$^{+/+}$ + LPS groups.

severely depleted brain 2-AG (Fig. 5*A*), AA (Fig. 5*B*), and PGE_2 (Fig. 5*C*) under basal control conditions. LPS treatment caused a modest, but significant increase in 2-AG (Fig. 5*A*), a reduction in AA (Fig. 5*B*), and a substantial increase in PGE_2 (Fig. 5*C*). The LPS-induced elevations in both 2-AG and PGE_2 were strongly suppressed in DH376- and DO34-treated mice and DAGLα$^{-/-}$ mice, but not DO53-treated mice. LPS treatment also increased brain cytokines, and this effect was significantly attenuated in DAGLα$^{-/-}$ mice (Fig. 5*D* and *SI Appendix*, Fig. S10). DH376- and DO34-treated mice also showed reductions in LPS-stimulated brain cytokines, but interpreting these effects proved complicated because the control probe DO53 also blocked brain cytokine production to a similar degree (Fig. 5*D* and *SI Appendix*, Fig. S10). These data could indicate that one or more of the off-targets shared by the DAGL inhibitors and DO53 also participate, along with DAGLα (as supported by studies in DAGLα$^{-/-}$ mice), in LPS-induced cytokine production, or that active metabolites of the inhibitors may suppress cytokines. Finally, we found that LPS-induced anapyrexia was substantially blunted in DH376- and DO34-treated mice (Fig. 5*E*) and DAGLα$^{-/-}$ mice (Fig. 5*F*), but not DO53-treated mice (Fig. 5*E*).

These results, when combined with previous findings (36, 39, 41), indicate that blockade of the principal 2-AG biosynthetic and degradation enzymes in the brain, DAGLα and MAGL, respectively, produces overlapping (reductions in brain prostaglandins and cytokines), but distinct (suppression versus enhancement of anapyrexia) effects on LPS-induced neuroinflammation.

Discussion

Endocannabinoids regulate synaptic activity throughout the CNS and impact diverse physiological and behavioral processes (42, 43). Inhibitors of enzymes that degrade endocannabinoids have proven useful for elucidating the neurobiological and behavioral effects caused by heightened endocannabinoid activity (44). It has been more challenging, however, to determine the biological impact of reducing endocannabinoid function caused in large part by a lack of selective and CNS-active inhibitors that can block endocannabinoid production in vivo. Although DAGLα$^{-/-}$ and DAGLβ$^{-/-}$ mice have provided valuable models for investigating the in vivo effects of disrupting endocannabinoid biosynthesis, DAGLα plays an important role in brain development (13) and chronic alterations in endocannabinoid tone can lead to substantial CB_1R adaptations in the CNS (45, 46) and peripheral tissues (47). The endocannabinoid system also cross-talks with several other bioactive lipid pathways (8, 48, 49). The extent to which this larger lipid network is dynamically regulated in the CNS by acute disruption of endocannabinoid synthesis remains unknown. Here we have addressed these important questions by developing two selective, centrally active irreversible DAGL inhibitors—DH376 and DO34—along with a structurally related control probe DO53. Key to development of these chemical probes was the use of both broad-spectrum and tailored ABPP probes for assessing selectivity and DAGL inhibition in vivo.

Administration of DH376 and DO34 to mice revealed that brain 2-AG content is rapidly and dramatically reduced following acute inactivation of DAGLs. Both inhibitors also produced near-complete blockade of cerebellar DSE and hippocampal DSI, two forms of CB_1R-mediated synaptic plasticity (20), following only a 30-min incubation in brain slices. These results provide strong

experimental support for an on-demand model of endocannabinoid biosynthesis (21) versus alternative hypotheses invoking 2-AG storage and release. We also used DAGL inhibitors and tailored activity probes to discover that DAGLα is a short half-life (<4 h) protein in the CNS. The factors that regulate DAGLα turnover in brain cells remain unknown, but previous studies have shown that DAGLα localization and activity are regulated by interacts with scaffolding proteins (50) and phosphorylation by CamKII (51). It is possible that such protein–protein interactions and posttranslational modifications (>30 phosphorylation sites have been identified in DAGLα; www.phosphosite.org/homeAction.do) regulate DAGLα half-life in brain cells. Endocannabinoid-mediated synaptic plasticity has also been shown to depend on transcription and translation in the postsynaptic neuron (52), which is consistent with our observation of rapid, ongoing production of new DAGLα protein (Fig. 3) that generates a strong, tonic flux of 2-AG in the brain (Fig. 4). Modulating the half-life of DAGLα may thus provide neurons with a mechanism to influence the magnitude and duration of 2-AG signaling and associated physiological processes, such as learning and memory, which have been shown to require protein synthesis and degradation (53).

That the profound reduction in 2-AG caused by DAGL inhibitors was accompanied by alterations in DAGs, arachidonic acid, prostaglandins, and other endocannabinoids (AEA) underscores the remarkable integration of lipid signaling networks in the brain and the key role that DAGLs play in orchestrating this cross-talk. Although we interpret that many of the lipid changes caused by DAGL inhibitors reflect the direct flux of substrate and products through interconnected metabolic pathways (19), others (e.g., AEA reductions) may be the indirect consequence of alterations in lipid signaling. Such signaling-related cross-talk between endocannabinoids has also been reported for AEA action on TRPV1 channels, which can influence 2-AG production in the brain (54). Regardless of the precise mechanisms by which DAGLs exert their profound influence over brain lipid networks, our data emphasize that the interpretation of phenotypes caused by DAGL disruption should take into consideration more than just impairments in endocannabinoid signaling. In this regard, our data, combined with previous studies (41, 55), suggest that the attenuated neuroinflammatory responses in DAGLα-disrupted mice likely reflect the integrated outcome of lowering both endocannabinoids and eicosanoids in the brain, although the additional impact of altering DAG-mediated PKC signaling or other lipid processes cannot be excluded. Additionally, our discovery that the control probe DO53 attenuates LPS-induced cytokine production without altering brain prostaglandins or anapyrexia indicates that the various neuroinflammatory effects of LPS can be mechanistically uncoupled.

Our studies, taken together, demonstrate that DH376 and DO34, along with the control probe DO53 and tailored DAGL activity probes, such as DH379 and HT-01, constitute a valuable chemical tool kit for studying diverse aspects of DAGL function and regulation both in animals and ex vivo brain preparations. Projecting forward, this tool kit would be further enhanced by the development of inhibitors that can selectively target DAGLα or DAGLβ. Although DO34 shows some preference for inhibiting DAGLα over DAGLβ in vivo, this window of selectivity is narrow and, conversely, centrally active DAGLβ-selective inhibitors are still lacking. Accordingly, even though studies with genetically disrupted mice (13, 14, 17) would indicate that most of the lipid changes caused by DAGL inhibitors in the brain are a result of blockade of DAGLα, we cannot, at this stage, exclude a contribution from DAGLβ in our pharmacological experiments, especially when evaluating the neuroinflammatory effects of DAGL inhibitors.

The short half-life of DAGLα also presents some challenges for our current set of inhibitors, because they need to be administered to mice at relatively high doses (50 mg/kg) to maintain complete target engagement over a prolonged (>8 h) period. Improving the pharmacokinetic properties of DAGLα inhibitors would thus benefit pharmacological studies aimed at studying prolonged inactivation of DAGLα in vivo. From a translational perspective, it will be interesting to determine which of the many phenotypes observed in DAGLα$^{-/-}$ mice are recapitulated in animals treated with DAGL inhibitors. The DAGLα$^{-/-}$ mice show reduced body weight caused by hypophagia and, in this regard, resemble animals with genetic or pharmacological disruption of the CB_1R (15). Humans treated with CB_1R antagonists/inverse agonists similarly exhibit weight loss, but these drugs were ultimately removed from the clinic because of neuropsychiatric side effects (56). DAGLα$^{-/-}$ mice also display heightened anxiety-related behaviors that can be normalized, along with partial restoration of brain 2-AG content, by treatment with an MAGL inhibitor (17). Thus, the potential clinical utility of DAGL inhibitors for obesity or other disorders (57–59) may depend on whether a therapeutic window can be established, within which partial reductions in endocannabinoid signaling are found to produce beneficial effects while minimizing untoward neurological outcomes. The DAGL inhibitors reported herein, which produce a graded, dose-dependent blockade of 2-AG production in the CNS, provide a first opportunity to experimentally investigate these important questions.

Materials and Methods

An extended section is provided in *SI Appendix, Supporting Experimental Procedures*. Animal experiments were conducted in accordance with the guidelines of the Institutional Animal Care and Use Committee of The Scripps Research Institute. Animal experiments performed at Leiden University were approved by the Local Ethics Committee under protocol number DEC 14137.

Chemical Synthesis and Characterization. DAGL inhibitor DH376 and DO34, and inactive control compound DO53 were synthesized and characterized as described in *SI Appendix, Supporting Experimental Procedures*.

Biochemical Studies. ABPP of mouse brain and substrate assays of transfected cell lysates were performed as described previously (27, 30). Metabolomic and proteomic analysis, as well as cytokine measurement from mouse brain homogenates were performed as described previously (60) and in *SI Appendix, Supporting Experimental Procedures*.

Electrophysiology. Preparation of mouse brain slices and recording of postsynaptic currents were performed as described previously (61) and in *SI Appendix, Supporting Experimental Procedures*.

LPS-Induced Anapyrexia. Induction of anapyrexia and measurement of mouse core body temperature were performed as described previously (62) and in *SI Appendix, Supporting Experimental Procedures*.

ACKNOWLEDGMENTS. We thank B. I. Florea and H. van den Elst for technical assistance, and K. L. Hsu for advice on inhibitor development. This work was supported by the National Institutes of Health Grants DA033760 (to B.F.C.), GM109315 (to A.V.), DA035217 and MH101146 (to Q.-s.L.); grants from the Chinese Scholarship Council (to H.D. and J.Z.); a Dutch Research Council–Chemical Sciences ECHO grant (to M.v.d.S.); and an ECHO-STIP Grant (to M.S. and M.v.d.S.).

1. Brady S, Siegel G, Albers RW, Price D (2012) *Basic Neurochemistry* (Academic, Waltham, MA), 8th Ed, pp 235–389.
2. Yung YC, Stoddard NC, Mirendil H, Chun J (2015) Lysophosphatidic acid signaling in the nervous system. *Neuron* 85(4):669–682.
3. Choi JW, Chun J (2013) Lysophospholipids and their receptors in the central nervous system. *Biochim Biophys Acta* 1831(1):20–32.
4. Katona I, Freund TF (2008) Endocannabinoid signaling as a synaptic circuit breaker in neurological disease. *Nat Med* 14(9):923–930.
5. Cimino PJ, Keene CD, Breyer RM, Montine KS, Montine TJ (2008) Therapeutic targets in prostaglandin E2 signaling for neurologic disease. *Curr Med Chem* 15(19):1863–1869.
6. Bryan L, Kordula T, Spiegel S, Milstien S (2008) Regulation and functions of sphingosine kinases in the brain. *Biochim Biophys Acta* 1781(9):459–466.

7. Choi SH, Aid S, Bosetti F (2009) The distinct roles of cyclooxygenase-1 and -2 in neuroinflammation: Implications for translational research. *Trends Pharmacol Sci* 30(4):174–181.
8. Reisenberg M, Singh PK, Williams G, Doherty P (2012) The diacylglycerol lipases: Structure, regulation and roles in and beyond endocannabinoid signalling. *Philos Trans R Soc Lond B Biol Sci* 367(1607):3264–3275.
9. Murataeva N, Straiker A, Mackie K (2014) Parsing the players: 2-arachidonoylglycerol synthesis and degradation in the CNS. *Br J Pharmacol* 171(6):1379–1391.
10. Bisogno T, et al. (2003) Cloning of the first sn1-DAG lipases points to the spatial and temporal regulation of endocannabinoid signaling in the brain. *J Cell Biol* 163(3): 463–468.
11. Mechoulam R, et al. (1995) Identification of an endogenous 2-monoglyceride, present in canine gut, that binds to cannabinoid receptors. *Biochem Pharmacol* 50(1):83–90.
12. Sugiura T, et al. (1995) 2-Arachidonoylglycerol: A possible endogenous cannabinoid receptor ligand in brain. *Biochem Biophys Res Commun* 215(1):89–97.
13. Gao Y, et al. (2010) Loss of retrograde endocannabinoid signaling and reduced adult neurogenesis in diacylglycerol lipase knock-out mice. *J Neurosci* 30(6):2017–2024.
14. Tanimura A, et al. (2010) The endocannabinoid 2-arachidonoylglycerol produced by diacylglycerol lipase alpha mediates retrograde suppression of synaptic transmission. *Neuron* 65(3):320–327.
15. Powell DR, et al. (2015) Diacylglycerol lipase α knockout mice demonstrate metabolic and behavioral phenotypes similar to those of cannabinoid receptor 1 knockout mice. *Front Endocrinol (Lausanne)* 6:86.
16. Jenniches I, et al. (April 14, 2015) Anxiety, stress, and fear response in mice with reduced endocannabinoid levels. *Biol Psychiatry*, 10.1016/j.biopsych.2015.03.033.
17. Shonesy BC, et al. (2014) Genetic disruption of 2-arachidonoylglycerol synthesis reveals a key role for endocannabinoid signaling in anxiety modulation. *Cell Reports* 9(5):1644–1653.
18. Whatley RE, Zimmerman GA, McIntyre TM, Prescott SM (1990) Lipid metabolism and signal transduction in endothelial cells. *Prog Lipid Res* 29(1):45–63.
19. Kohnz RA, Nomura DK (2014) Chemical approaches to therapeutically target the metabolism and signaling of the endocannabinoid 2-AG and eicosanoids. *Chem Soc Rev* 43(19):6859–6869.
20. Kano M, Ohno-Shosaku T, Hashimotodani Y, Uchigashima M, Watanabe M (2009) Endocannabinoid-mediated control of synaptic transmission. *Physiol Rev* 89(1): 309–380.
21. Hashimotodani Y, et al. (2013) Acute inhibition of diacylglycerol lipase blocks endocannabinoid-mediated retrograde signalling: Evidence for on-demand biosynthesis of 2-arachidonoylglycerol. *J Physiol* 591(Pt 19):4765–4776.
22. Min R, et al. (2010) Diacylglycerol lipase is not involved in depolarization-induced suppression of inhibition at unitary inhibitory connections in mouse hippocampus. *J Neurosci* 30(7):2710–2715.
23. Zhang L, Wang M, Bisogno T, Di Marzo V, Alger BE (2011) Endocannabinoids generated by Ca2+ or by metabotropic glutamate receptors appear to arise from different pools of diacylglycerol lipase. *PLoS One* 6(1):e16305.
24. Bisogno T, et al. (2013) A novel fluorophosphonate inhibitor of the biosynthesis of the endocannabinoid 2-arachidonoylglycerol with potential anti-obesity effects. *Br J Pharmacol* 169(4):784–793.
25. Baggelaar MP, et al. (2015) Highly selective, reversible inhibitor identified by comparative chemoproteomics modulates diacylglycerol lipase activity in neurons. *J Am Chem Soc* 137(27):8851–8857.
26. Hoover HS, Blankman JL, Niessen S, Cravatt BF (2008) Selectivity of inhibitors of endocannabinoid biosynthesis evaluated by activity-based protein profiling. *Bioorg Med Chem Lett* 18(22):5838–5841.
27. Hsu KL, et al. (2012) DAGLβ inhibition perturbs a lipid network involved in macrophage inflammatory responses. *Nat Chem Biol* 8(12):999–1007.
28. Baggelaar MP, et al. (2013) Development of an activity-based probe and in silico design reveal highly selective inhibitors for diacylglycerol lipase-α in brain. *Angew Chem Int Ed Engl* 52(46):12081–12085.
29. Niphakis MJ, Cravatt BF (2014) Enzyme inhibitor discovery by activity-based protein profiling. *Annu Rev Biochem* 83:341–377.
30. van der Wel T, et al. (2015) A natural substrate-based fluorescence assay for inhibitor screening on diacylglycerol lipase α. *J Lipid Res* 56(4):927–935.
31. Rostovtsev VV, Green LG, Fokin VV, Sharpless KB (2002) A stepwise huisgen cycloaddition process: Copper(I)-catalyzed regioselective "ligation" of azides and terminal alkynes. *Angew Chem Int Ed Engl* 41(14):2596–2599.
32. Patricelli MP, Giang DK, Stamp LM, Burbaum JJ (2001) Direct visualization of serine hydrolase activities in complex proteomes using fluorescent active site-directed probes. *Proteomics* 1(9):1067–1071.
33. Liu Y, Patricelli MP, Cravatt BF (1999) Activity-based protein profiling: The serine hydrolases. *Proc Natl Acad Sci USA* 96(26):14694–14699.
34. Wilson-Grady JT, Haas W, Gygi SP (2013) Quantitative comparison of the fasted and re-fed mouse liver phosphoproteomes using lower pH reductive dimethylation. *Methods* 61(3):277–286.
35. Marignani PA, Epand RM, Sebaldt RJ (1996) Acyl chain dependence of diacylglycerol activation of protein kinase C activity in vitro. *Biochem Biophys Res Commun* 225(2): 469–473.
36. Nomura DK, et al. (2011) Endocannabinoid hydrolysis generates brain prostaglandins that promote neuroinflammation. *Science* 334(6057):809–813.
37. Kita Y, et al. (2015) Fever is mediated by conversion of endocannabinoid 2-arachidonoylglycerol to prostaglandin E2. *PLoS One* 10(7):e0133663.
38. Pasquarelli N, et al. (2015) Comparative biochemical characterization of the monoacylglycerol lipase inhibitor KML29 in brain, spinal cord, liver, spleen, fat and muscle tissue. *Neuropharmacology* 91:148–156.
39. Viader A, et al. (2015) Metabolic interplay between astrocytes and neurons regulates endocannabinoid action. *Cell Reports* 12(5):798–808.
40. Steiner AA, et al. (2011) The hypothermic response to bacterial lipopolysaccharide critically depends on brain CB1, but not CB2 or TRPV1, receptors. *J Physiol* 589(Pt 9): 2415–2431.
41. Nass SR, et al. (2015) Endocannabinoid catabolic enzymes play differential roles in thermal homeostasis in response to environmental or immune challenge. *J Neuroimmun Pharmacol* 10(2):364–370.
42. Mechoulam R, Parker LA (2013) The endocannabinoid system and the brain. *Annu Rev Psychol* 64:21–47.
43. Fowler CJ (2015) The potential of inhibitors of endocannabinoid metabolism as anxiolytic and antidepressive drugs—A practical view. *Eur Neuropsychopharmacol* 25(6): 749–762.
44. Blankman JL, Cravatt BF (2013) Chemical probes of endocannabinoid metabolism. *Pharmacol Rev* 65(2):849–871.
45. Schlosburg JE, et al. (2010) Chronic monoacylglycerol lipase blockade causes functional antagonism of the endocannabinoid system. *Nat Neurosci* 13(9):1113–1119.
46. Chanda PK, et al. (2010) Monoacylglycerol lipase activity is a critical modulator of the tone and integrity of the endocannabinoid system. *Mol Pharmacol* 78(6):996–1003.
47. Taschler U, et al. (2015) Monoglyceride lipase deficiency causes desensitization of intestinal cannabinoid receptor type 1 and increased colonic μ-opioid receptor sensitivity. *Br J Pharmacol* 172(17):4419–4429.
48. Piomelli D (2014) More surprises lying ahead. The endocannabinoids keep us guessing. *Neuropharmacology* 76 Pt B:228–234.
49. Fowler CJ, Naidu PS, Lichtman A, Onnis V (2009) The case for the development of novel analgesic agents targeting both fatty acid amide hydrolase and either cyclooxygenase or TRPV1. *Br J Pharmacol* 156(3):412–419.
50. Jung KM, et al. (2007) A key role for diacylglycerol lipase-alpha in metabotropic glutamate receptor-dependent endocannabinoid mobilization. *Mol Pharmacol* 72(3): 612–621.
51. Shonesy BC, et al. (2013) CaMKII regulates diacylglycerol lipase-α and striatal endocannabinoid signaling. *Nat Neurosci* 16(4):456–463.
52. Yuan S, Burrell BD (2013) Endocannabinoid-dependent long-term depression in a nociceptive synapse requires coordinated presynaptic and postsynaptic transcription and translation. *J Neurosci* 33(10):4349–4358.
53. Bingol B, Sheng M (2011) Deconstruction for reconstruction: The role of proteolysis in neural plasticity and disease. *Neuron* 69(1):22–32.
54. Maccarrone M, et al. (2008) Anandamide inhibits metabolism and physiological actions of 2-arachidonoylglycerol in the striatum. *Nat Neurosci* 11(2):152–159.
55. Choi SH, Langenbach R, Bosetti F (2008) Genetic deletion or pharmacological inhibition of cyclooxygenase-1 attenuate lipopolysaccharide-induced inflammatory response and brain injury. *FASEB J* 22(5):1491–1501.
56. Kirilly E, Gonda X, Bagdy G (2012) CB1 receptor antagonists: New discoveries leading to new perspectives. *Acta Physiol (Oxf)* 205(1):41–60.
57. Busquets-Garcia A, et al. (2013) Targeting the endocannabinoid system in the treatment of fragile X syndrome. *Nat Med* 19(5):603–607.
58. Bashashati M, et al. (2015) Inhibiting endocannabinoid biosynthesis: A novel approach to the treatment of constipation. *Br J Pharmacol* 172(12):3099–3111.
59. Oleson EB, et al. (2012) Endocannabinoids shape accumbal encoding of cue-motivated behavior via CB1 receptor activation in the ventral tegmentum. *Neuron* 73(2): 360–373.
60. Inloes JM, et al. (2014) The hereditary spastic paraplegia-related enzyme DDHD2 is a principal brain triglyceride lipase. *Proc Natl Acad Sci USA* 111(41):14924–14929.
61. Pan B, et al. (2009) Blockade of 2-arachidonoylglycerol hydrolysis by selective monoacylglycerol lipase inhibitor 4-nitrophenyl 4-(dibenzo[d][1,3]dioxol-5-yl(hydroxy)methyl)piperidine-1-carboxylate (JZL184) Enhances retrograde endocannabinoid signaling. *J Pharmacol Exp Ther* 331(2):591–597.
62. Conti B, et al. (2006) Transgenic mice with a reduced core body temperature have an increased life span. *Science* 314(5800):825–828.